Communication

Quasi-Isotropic Radiation Pattern Synthesis Using Triple Current Line Sources

Peiqin Liu and Yue Li

***Abstract*— This communication proposes a design method to synthesize a quasi-isotropic radiation pattern with a planar antenna structure. The proposed method is based on the combination of triple current line sources. As a demonstrated example, a pair of out-of-phase line sources is combined with another orthogonal line source for radiation pattern synthesis. By optimizing the spatial distance in the proposed triple current line source model, quasi-isotropic radiation performance can be realized with theoretical analyses, showing that the gain variation (i.e., the maximum gain minuses the minimum gain) of the proposed method is 0.53 dB. As a proof of concept, a folded dipole antenna is designed and fabricated to verify the proposed method. Full-wave simulation shows the gain variation of the folded dipole antenna is 1.37 dB and measured result is 3.62 dB.**

***Index Terms*— Antenna radiation patterns, pattern synthesis, quasi-isotropic antennas, triple line source combination.**

I. Introduction

An isotropic source is a theoretical radiator, which radiates the same intensity of radiation in all directions [1]–[3]. In electromagnetic and antenna theory, the concept of isotropic source is quite significant, because it benchmarks the radiation performance of radiators. In engineering applications, the isotropic radiator is also useful and provides uniform coverage in nondirectional beacon systems. However, according to the hairy ball theorem, any continuous tangent vector field on a sphere must vanish somewhere [4], [5]. From this conclusion, the electromagnetic wave, which is the transverse vector in far-field [6], cannot achieve perfect isotropic radiation pattern. To solve this problem, several methods are proposed to design the antenna with a quasi-isotropic radiation pattern. One method is designing antennas with tridimensional structures to realize quasi-isotropic coverage [7]–[11]. Using a tridimensional structure to design a quasi-isotropic antenna is a quite intuitive idea. However, the geometries of tridimensional antennas are relatively complicated.

Quasi-isotropic antennas with planar structures have drawn lots of attention due to the merits of low profile and easy fabrication [12]–[14]. An effective method to design a quasi-isotropic antenna is using crossed dipoles [12], [13]. By introducing phase difference in feeding ports, the dipole antennas can achieve a wide operating band for quasi-isotropic coverage with measured gain variation (the maximum gain minuses the minimum gain) less than 6 dB [13].

Manuscript received January 28, 2020; revised March 31, 2020; accepted May 9, 2020. Date of publication May 22, 2020; date of current version December 17, 2020. This work was supported in part by the Natural Science Foundation of Beijing Manipulate under Contract 4182029 and in part by the Youth Top Program of Beijing Outstanding Talent Funding Project. *(Corresponding author: Yue Li.)*

Peiqin Liu was with the Department of Electronic Engineering, Tsinghua University, Beijing 100084, China. He is now with the Department of Electrical and Computer Engineering, National University of Singapore, Singapore 117583 (e-mail: eleliup@nus.edu.sg).

Yue Li is with the Department of Electronic Engineering, Tsinghua University, Beijing 100084, China, and also with the Beijing National Research Center for Information Science and Technology (BNRist), Tsinghua University, Beijing 100084, China (e-mail: lyee@tsinghua.edu.cn).

Color versions of one or more of the figures in this communication are available online at https://ieeexplore.ieee.org.

Digital Object Identifier 10.1109/TAP.2020.2995299

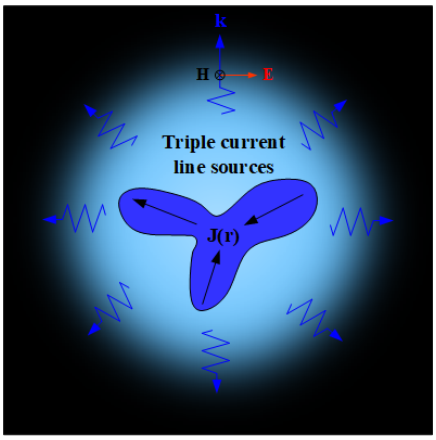

Fig. 1. General scenario of the proposed antenna in aircraft applications.

In radio frequency identification (RFID) applications, researchers utilize dipole antenna and complementary dipoles with modified structures to design planar quasi-isotropic antenna [14], [15]. Besides these antennas, an important method to design a quasi-isotropic antenna with a planar structure is using U-shaped dipole structures [16]–[18]. The U-shaped dipole antenna has a simple configuration. It consists of two vertical arms, which operate in $\lambda/4$ resonant mode and the currents are out of phase. The distance between the two arms is much less than the length of the arm [17]. As a result, the U-shaped antenna can realize quasi-isotropic radiation performance. Based on this method, researchers also propose patch antenna [22] and magnetic dipole antenna [23] for quasi-isotropic coverage applications.

In this communication, a quasi-isotropic radiation pattern synthesis method is proposed based on triple current line sources. In this method, three current line sources are arranged together to realize quasi-isotropic radiation. A conceptual sketch of the radiation pattern synthesis method is depicted in Fig. 1, showing that a triple-source combination with an optimized phase difference can achieve quasi-isotropic radiation for transversal vector waves. The proposed method is verified through theoretical analyses, numerical simulations, and experiments. Theoretical analyses show that the gain variation of the proposed method is 0.53 dB, which is an excellent result and quite close to ideal isotropic radiation. As a proof of concept, a planar quasi-isotropic folded dipole antenna is designed and fabricated to verify the proposed method. Although the proposed folded dipole has a similar structure with the U-shaped dipole antenna [19]–[21], there are some key differences between the U-shaped antenna and the proposed antenna. In the U-shaped antenna, the arms of the antenna are closely put together. Distance between the arms is $0.07\lambda_0$ in [20] and $0.14\lambda_0$ in [21] (λ_0 is the wavelength in free space). While the distance in the proposed folded antenna is $0.23\lambda_0$. Besides the geometry differences, the radiation mechanisms are different. In the U-shaped antenna, the currents flowing through the arms are canceled out in far-field and only the

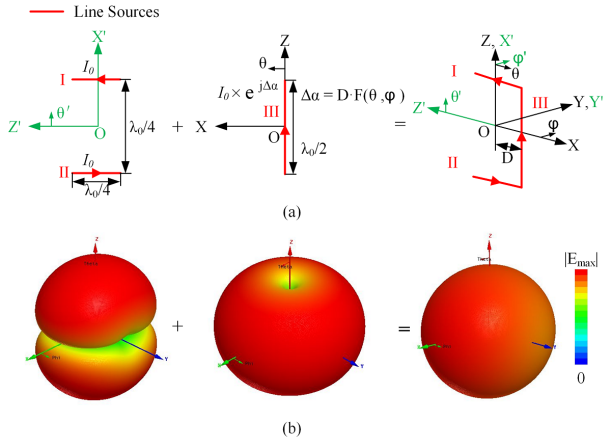

Fig. 2. Schematic of the theoretical model. (a) Pair of out-of-phase current sources is combined with another orthogonal current source with a phase difference of $\Delta\alpha$ due to spatial separation. λ_0 is the wavelength at the fixed frequency of f_0. (b) Radiation patterns according to the scheme in (a).

electric small current in the bottom of the antenna contributes to quasi-isotropic radiation [19]. The proposed method is based on a triple current line sources model. All of the three currents contribute to radiation and the quasi-isotropic performance can be achieved by optimizing the spatial distance between the current sources. Detailed theoretical analyses are derived in this communication, which shows a novel mechanism for quasi-isotropic radiation synthesis. Full-wave simulations show that the gain variation of the proposed antenna is 1.37 dB and the measured gain variation is 3.62 dB. The results exhibit a promising path for engineering quasi-isotropic coverage of electromagnetic waves in 3-D spherical space.

II. Theoretical Analyses for Triple Current Line Sources Method

In this section, a feasible and particular configuration using a triple current line sources model is proposed as shown in Fig. 2 to analyze the performance of the proposed method. The theoretical model is composed of three uniform current sources with tailorable phase differences. Fig. 2(a) depicts the positions of the three currents, which can be divided into two components. One component is a pair of out-of-phase current sources positioning along z' -axis (in the x' –y' –z' coordinate system) and the other is a single current source positioning along z-axis (in the x–y–z coordinate system). There is a spatial separation of D between the two components. The coordinate systems x–y–z and x'–y'–z' share the same $y(y')$-axis, but differ on a 90° rotation around it. The physical mechanism behind this configuration is that the spatial distance D between the line sources would provide a phase difference of $\Delta\alpha$, which is a key parameter to achieve quasi-isotropic radiation. The radiation patterns of each component are plotted in Fig. 2(b). For the current pair (lines sources I and II), a bidirectional radiation pattern is achieved in $+z(+x')$- and $-z(-x')$ -axis. For the single current source (line source III), an omnidirectional radiation pattern is achieved in xy plane, with nulls in $+z$- and $-z$-axis. Thus, the two components have the potential to complement each other and achieve quasi-isotropic radiation. The synthesized radiation pattern is plotted in the right of Fig. 2(b), confirming a nearly isotropic radiation performance.

In order to quantitatively evaluate the isotropic properties of the proposed method, electric fields in far-field [17]–[19] are derived as follows. The length of line sources I and II is $\lambda_0/4$ and the length of line source III is $\lambda_0/2$. There is a distance, represented by parameter D, between the line source III and the origin of the coordinates, represented by the point O. It is assumed that the current in the line sources is distributed uniformly and the amplitude is I_0. The far-field components of line source I [19] are given by

$$\begin{aligned} E_{I\theta'} &= \int_{-\frac{\lambda}{8}}^{\frac{\lambda}{8}} dE' e^{j\Delta\alpha'} \\ &= \left(j\frac{\eta_0 I_0 e^{-j\beta r'}}{2\lambda r'\beta}\right)\left(2\tan\theta'\sin\left(\frac{\pi}{4}\cos\theta'\right)\right) e^{j\frac{\pi}{2}\cos\varphi'\sin\theta'} \\ E_{I\varphi'} &= 0 \end{aligned} \tag{1}$$

where $\Delta\alpha'$ is the phase introduced by the distance between line source I and the original point O. Similarly, the far-field components of line source II are given by

$$\begin{aligned} E_{II\theta'} &= \left(j\frac{\eta_0 I_0 e^{-j\beta r'}}{2\lambda r'\beta}\right)\left(-2\tan\theta'\sin\left(\frac{\pi}{4}\cos\theta'\right)\right) e^{-j\frac{\pi}{2}\cos\varphi'\sin\theta'} \\ E_{II\varphi'} &= 0. \end{aligned} \tag{2}$$

Line source III locates in the x–y–z coordinate system and the far-field components of line source III are given by

$$\begin{aligned} E_{III\theta} &= \int_{-\frac{\pi}{4}}^{\frac{\pi}{4}} dE e^{j\Delta\alpha} \\ &= \left(j\frac{\eta_0 I_0 e^{-j\beta r}}{2\lambda r\beta}\right)\left(2\tan\theta\sin\left(\frac{\pi}{2}\cos\theta\right)\right) e^{j\beta D\cos\varphi\sin\theta} \\ E_{III\varphi} &= 0 \end{aligned} \tag{3}$$

where $\Delta\alpha$ is the phase introduced by distance D between line source III and the original point O in the x–y–z coordinate system. Then, the total electric field can be derived as

$$\begin{aligned} E_{\text{Tol}} &= \sqrt{\left|E_\theta^2\right| + \left|\mathrm{E}_\varphi^2\right|} \\ E_\theta &= \widehat{\theta}\cdot\overrightarrow{E_{I\theta'}} + \widehat{\theta}\cdot\overrightarrow{\mathrm{E}_{II\theta'}} + E_{III\theta} \\ &= \widehat{\theta}\cdot\widehat{\theta}'E_{I\theta'} + \widehat{\theta}\cdot\widehat{\theta}'E_{II\theta'} + E_{III\theta} \\ E_\varphi &= \widehat{\varphi}\cdot\overrightarrow{E_{I\theta'}} + \widehat{\varphi}\cdot\overrightarrow{E_{II\theta'}} + E_{III\varphi} \\ &= \widehat{\varphi}\cdot\widehat{\theta}'E_{I\theta'} + \widehat{\varphi}\cdot\widehat{\theta}'E_{II\theta'}. \end{aligned} \tag{4}$$

It should be noted that there are two coordinate systems, i.e., x–y–z and x'–y'–z', in the expression. Thus, coordinate transformations are utilized to find the relationship between the two coordinate systems and the relationship is derived as

$$\begin{aligned} \theta' &= \arccos(-\sin\theta\cos\varphi) \\ \varphi' &= \text{angle}(\cos\theta + j\sin\theta\sin\varphi) \\ \widehat{\theta}\cdot\widehat{\theta}' &= -\cos\theta'\cos\varphi'\sin\theta + \cos\theta'\sin\varphi'\cos\theta\sin\varphi \\ &\quad + \sin\theta'\cos\theta\cos\varphi \\ \widehat{\varphi}\cdot\widehat{\theta}' &= \cos\theta'\sin\varphi'\cos\varphi - \sin\theta'\sin\varphi. \end{aligned} \tag{5}$$

Substituting (1)–(3), and (5) into (4), the gain variation of the total electric field can be quantitatively calculated. Fig. 3 depicts the calculated gain variation results of the proposed triple current line sources method. As shown in Fig. 3(a), the gain variation of the proposed model is a function of the spatial distance D (for a fixed operating frequency of f_0), as well as a function of the operating frequency f_0 (for a fixed separation distance D), corresponding to the blue and red curves, respectively. It can be concluded from the blue curve that an optimal gain variation result of 0.53 dB can be obtained for $D = \lambda_0/8$ (λ_0 is the wavelength at the fixed frequency of f_0), thus achieving quasi-isotropic radiation property in the full space.

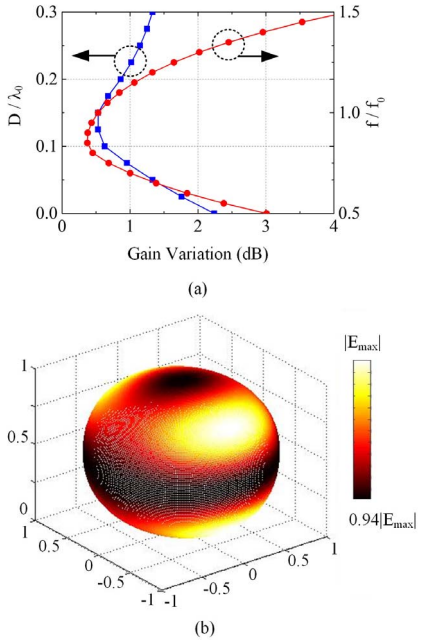

Fig. 3. Isotropic property analyses. (a) Gain variation, i.e., the difference between the maximum and minimum gain, in full space with different separated distance of D at f_0 (the blue curve) and different operating frequency f (the red curve with D fixed as $\lambda_0/8$). (b) 3-D radiation pattern of the theoretical model in Fig.2 with D fixed as $\lambda_0/8$ at f_0.

In order to assess the bandwidth of quasi-isotropic radiation, the red curve in Fig. 3(a) represents the gain variations for $D = \lambda_0/8$ as a function of the operating frequency. These results demonstrate that the gain variations are less than 3 dB within a fractional bandwidth of 95%. Therefore, the triple current line sources model is inherently broadband. To clearly show the small deviations between a perfect isotropic pattern and the radiation of the proposed method, Fig. 3(b) represents the 3-D radiation pattern at the central frequency f_0 with $D = \lambda_0/8$. The axis of the electric field is scaled from $0.94|E_{\max}|$ to $|E_{\max}|$, which presents the quasi-isotropic radiation performance of the proposed line source optimization method.

III. Antenna Design

These theoretical analyses demonstrate that the proposed triple current line sources method is feasible for the synthesis of quasi-isotropic radiation. The method has been presented at a generic frequency f_0 and could be implemented in different frequency regimes and physical platforms. In this section, a proof-of-concept experimental demonstration is provided at microwave frequency to verify the proposed method. As illustrated in Fig. 4, the proposed antenna has a folded dipole configuration based on FR4 ($\varepsilon_r = 4.4$) substrate. This configuration is proposed since this structure provides three current elements similar to those of the theoretical model and it can be easily excited by one feeding port. The main difference between the theoretical model and the folded dipole antenna is that in our prototype as shown in Fig. 4, the current pair, i.e., current I and II, supports the quarter-wavelength mode, which is different from the ideal uniform current in the theoretical model shown in Fig. 2(a). On the other hand, the current in current III is almost uniform, which is closer to the theoretical model in Fig. 2(a). The structure used in the folded dipole prototype also has two practical advantages: First, three current sources are provided in a single structure with known modes and current distributions and second, excitation and measurement of the folded dipole antenna is relatively simple.

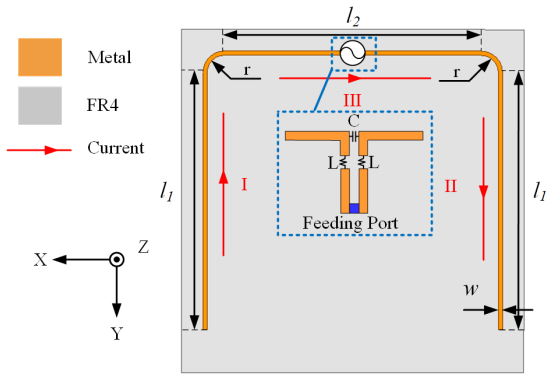

Fig. 4. Geometry of the proposed folded dipole antenna. Detailed parameters: $l_1 = 60$ mm, $l_2 = 60$ mm, $r = 4$ mm, $w = 1$ mm, $L = 24$ nH, and $C = 0.5$ pF.

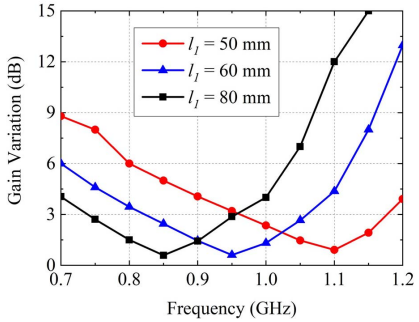

Fig. 5. Simulated gain variations with different values of (a) l_1 and (b) l_2.

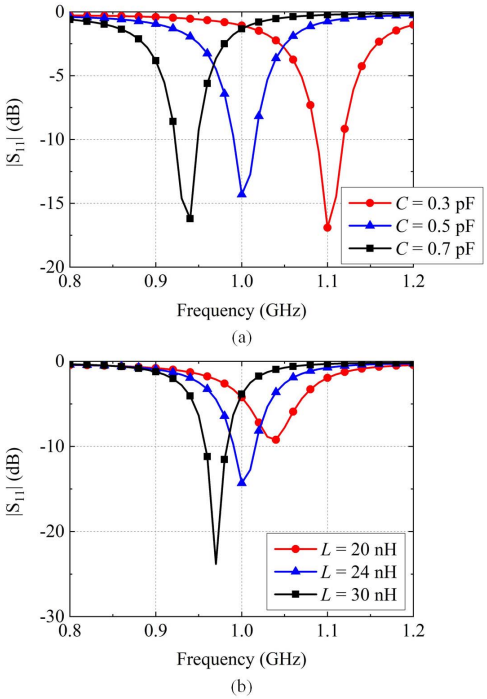

Fig. 6. Simulated $|S_{11}|$ of the proposed folded dipole antenna with different values of (a) capacitance C and (b) inductance L.

The parameter study of the proposed folded dipole antenna is shown in Figs. 5 and 6. Fig. 5 depicts the simulated results of gain variation with different values of l_1. When the value of l_1

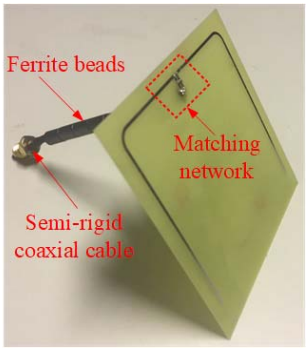

Fig. 7. Photograph of the proposed folded dipole antenna.

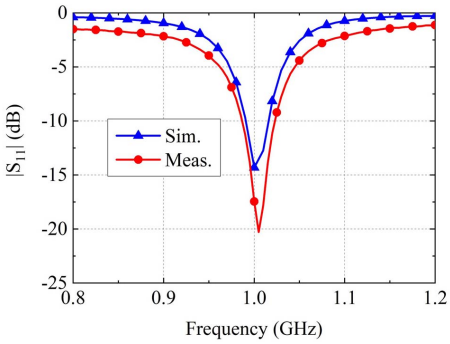

Fig. 8. Simulated and measured $|S_{11}|$ of the proposed antenna.

is 50 mm, the gain variation of the proposed antenna is less than 3 dB in the frequency range from 0.96 to 1.18 GHz and the minimum gain variation is 0.59 dB at 0.85 GHz. As l_1 increases from 50 to 80 mm, the operating frequency band with quasi-isotropic radiation performance would shift to lower frequency.

The whole length of the proposed folded dipole antenna is larger than half wavelength. A matching network, as shown in Fig. 4, is necessary to match the proposed antenna at the desired frequency. In the matching network, a small piece of parallel line transmission line is extended from the folded dipole antenna. A capacitor is connected between the two arms of the folded dipole antenna and a pair of inductors is cascaded in the transmission line. With the matching network, the operating frequency of the proposed antenna can be optimized by tuning the values of the capacitor and inductors. Fig. 6 illustrates the simulated $|S_{11}|$ results of the proposed antenna with different values of capacitance and inductance. As shown in Fig. 6(a), when the value of C is 0.3 pF, the proposed antenna operates at 1.1 GHz. As the capacitance increases to 0.5 pF, the operating frequency is tuned to the desired frequency band of 1 GHz. When the capacitance further increases to 0.7 pF, the operating frequency decreases to 0.94 GHz. Fig. 6(b) depicts the simulated $|S_{11}|$ results with different values of inductance L. When the value of L is 20 nH, the minimum reflection coefficient of the proposed antenna is -9.2 dB at 1.04 GHz. As the value of L increases from 20 to 30 nH, the operating frequency band shifts to lower band and the impedance mismatch is also improved. In this communication, all of the abovementioned full-wave simulations are carried out by commercial software ANSYS high-frequency structure simulator (HFSS) version 18 [24].

IV. Experimental Results

A prototype of the proposed folded dipole antenna is fabricated and tested to verify the design strategy. Fig. 7 shows the photograph of the proposed antenna. The antenna is designed and fabricated with FR4 ($\varepsilon_r = 4.4$) substrate. A semirigid coaxial cable is utilized to excite the folded dipole antenna. Ferrite beads operate as RF choke to mitigate the current on the cable [25]. It should be noted that the proposed antenna achieves quasi-isotropic radiation by optimizing the spatial distance between currents. Compared with U-shaped antennas [19]–[21], the proposed antenna occupies larger space.

The simulated and measured $|S_{11}|$ results of the proposed antenna are shown in Fig. 8. The results are measured by vector network analyzer E5071B. The simulated -10 dB bandwidth is 0.99–1.02 GHz. The measured bandwidth is slightly broader than the simulated result because the chip capacitor and inductor introduce some loss, which decreases the Q factor of the proposed folded dipole antenna.

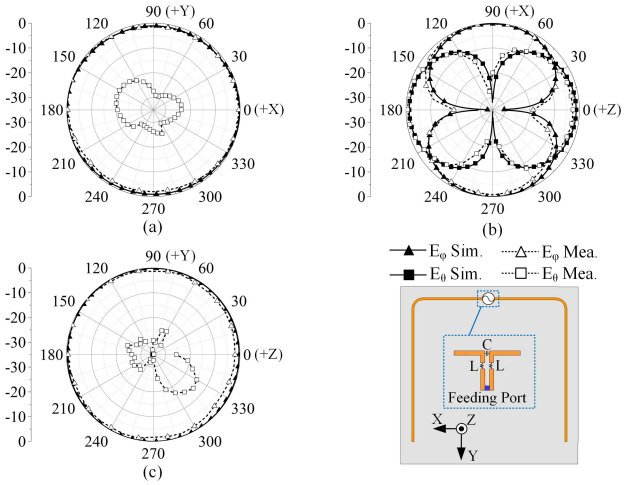

Fig. 9. Simulated and measured radiation patterns of the proposed antenna at 1 GHz. (a) *xoy* plane ($\theta = 90°$). (b) *xoz* plane ($\varphi = 0°$). (c) *yoz* plane ($\varphi = 90°$).

To verify the quasi-isotropic radiation performance, the simulated and measured radiation patterns of the proposed antenna in the three principal planes at 1 GHz are shown in Fig. 9. One can observe that the measured results match well with simulation. In *xoy* plane and *yoz* plane, the E_θ component exhibits omnidirectional radiation patterns, while the E_φ component is quite small. Fig. 9(a) and (c) shows that the simulated gain variation of the E_θ component is 1.15 dB and the measured result is 2.92 dB. The simulated results of the E_φ component are less than -34 dB, which is too small to be shown in the figures. The measured results of the E_φ component are less than -19.19 dB in the *xoy* plane and less than -14.64 dB in the *yoz* plane. Fig. 9(b) shows the radiation patterns in the *xoz* plane. In this plane, the E_θ component and E_φ component compensate with each other, which makes the total electric fields a quasi-isotropic radiation performance. Normalized gain contour lines of the proposed antenna at 1 GHz are depicted in Fig. 10. As shown in Fig. 10(a), the simulated gain variation of the proposed antenna is 1.37 dB in full space. Fig. 10(b) shows the measured results of gain variation. The measured gain contour lines match well with simulation and the measured gain variation is 3.62 dB. Fig. 11 shows the relationship between gain variation and operating frequency. The simulated gain variation is less than 3 dB from 0.83 to 1.06 GHz. The measured gain variation is less than 6 dB from 0.84 to 1.04 GHz. Although the isotropic radiation performance deteriorates in measurement due to fabrication and measurement tolerance, the performance is still acceptable for isotropic coverage in practical applications [12], [13].

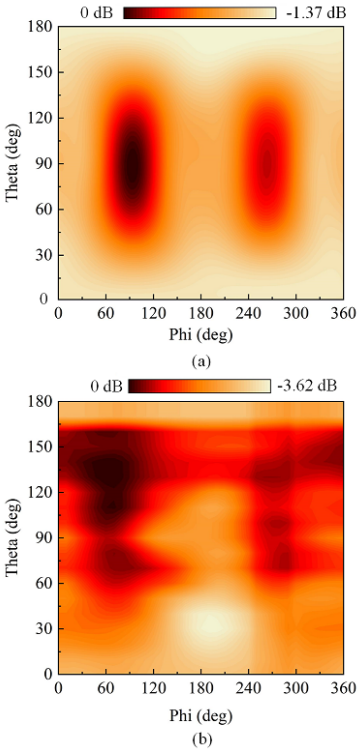

Fig. 10. Normalized gain contour lines of the proposed antenna at 1 GHz. (a) Simulated results. (b) Measured results.

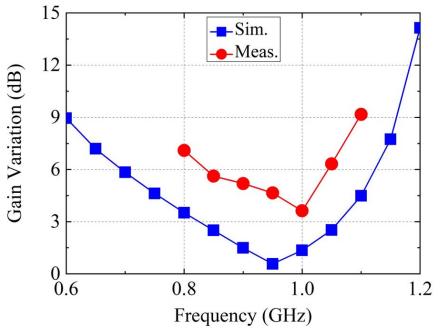

Fig. 11. Simulated and measured gain variation of the proposed antenna.

It should be noted that there are some deviations between the simulated and measured results in Fig. 11. This phenomenon is caused by the feeding cable and ferrite beads in the experiment. In practical applications, the cable and ferrite beads can be removed, which would further improve the measurement results. Fig. 12 shows the simulated and measured realized gain of the proposed folded dipole antenna. At the center frequency of 1 GHz, the simulated peak gain is 0.58 dBi and the measured result is −0.90 dBi. The deviations between the simulated and measured results are caused by measurement tolerance and loss of the matching network.

A comparison is tabulated in Table I to compare the performance of the proposed method with other quasi-isotropic antennas. The proposed antenna is designed based on a triple current line sources model. A folded dipole is proposed to verify the triple current line sources model. The measured gain variation of the proposed folded dipole antenna is 3.62 dB. One can observe that the proposed triple current line sources method presents the best quasi-isotropic radiation performance. It should be noted that there is a tradeoff between

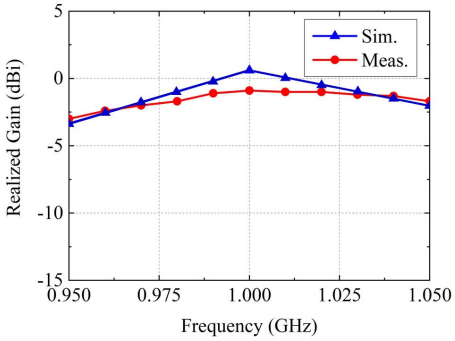

Fig. 12. Simulated and measured gain of the proposed antenna.

TABLE I
COMPARISONS OF QUASI-ISOTROPIC ANTENNAS

Reference	Structure	Principle of operation	Gain variation (dB)
[9]	3D	Complementary dipoles	5.2
[10]	3D	Complementary dipoles	5.6
[15]	3D	Complementary dipoles	6.0
[23]	3D	Magnetic dipole	5.7
[11]	3D	Folded meander line	8.9
[12]	Planar	Cross dipoles	6.6
[13]	Planar	Cross dipoles	5.8
[14]	Planar	Folded meander line	6.0
This work	**Planar**	**Triple current line sources**	**3.6**

bandwidth and isotropic radiation performance and the bandwidth of the proposed folded dipole antenna can be increased by optimizing the dimensions of the antenna.

V. CONCLUSION

In this communication, a general design method is proposed to synthesize quasi-isotropic radiation with triple current line sources. To this end, a pair of out-of-phase line sources and a single line source are combined together. The single line source is separated with a distance from the out-of-phase current pair to provide a phase difference, which is a key parameter for quasi-isotropic radiation synthesis. Theoretical analyses show that the minimum gain variation of the proposed method is 0.53 dB. Moreover, a proof-of-concept experimental prototype is presented to verify the design strategy. The proposed prototype is a folded dipole antenna and operates at a microwave frequency band. Full-wave simulation demonstrates that the gain variation of the folded dipole is 1.37 dB and the measured one is 3.62 dB. The results show that the proposed method is quite promising in full spatial antenna coverage applications.

REFERENCES

[1] I. Liberal, I. Ederra, and Y. Li, "Isotropic single-photo sources," *Opt. Lett.*, vol. 4, no. 12, pp. 2736–2739, 2018.
[2] U. Sayin, P. Artís, and O. Guasch, "Realization of an omnidirectional source of sound using parametric loudspeakers," *J. Acoust. Soc. Amer.*, vol. 134, no. 3, pp. 1899–1907, Sep. 2013.
[3] T. W. Leishman, S. Rollins, and H. M. Smith, "An experimental evaluation of regular polyhedron loudspeakers as omnidirectional sources of sound," *J. Acoust. Soc. Amer.*, vol. 120, no. 3, pp. 1411–1422, Sep. 2006.
[4] M. Eisenberg and R. Guy, "A proof of the hairy ball theorem," *Amer. Math. Monthly*, vol. 86, no. 7, pp. 571–574, Aug. 1979.
[5] H. F. Mathis, "A short proof that an isotropic antenna is impossible," *Proc. IRE*, vol. 39, no. 8, p. 970, 1951.
[6] J. Vanderlinde, "Electromagnetic radiation," in *Classical Electromagnetic Theory*, 2ed ed. New York, NY, USA: Springer, pp. 269–311, 2005.

[7] S. Long, "A combination of linear and slot antennas for quasi-isotropic coverage," *IEEE Trans. Antennas Propag.*, vol. AP-23, no. 4, pp. 572–576, Jul. 1975.
[8] A. Mehdipour, H. Aliakbarian, and J. Rashed-Mohassel, "A novel electrically small spherical wire antenna with almost isotropic radiation pattern," *IEEE Antennas Wireless Propag. Lett.*, vol. 7, pp. 396–399, 2008.
[9] J.-H. Kim and S. Nam, "A compact quasi-isotropic antenna based on folded split-ring resonators," *IEEE Antennas Wireless Propag. Lett.*, vol. 16, pp. 294–297, 2017.
[10] Y.-M. Pan, K. W. Leung, and K. Lu, "Compact quasi-isotropic dielectric resonator antenna with small ground plane," *IEEE Trans. Antennas Propag.*, vol. 62, no. 2, pp. 577–585, Feb. 2014.
[11] Z. Su, K. Klionovski, R. M. Bilal, and A. Shamim, "A dual band additively manufactured 3-D antenna on package with near-isotropic radiation pattern," *IEEE Trans. Antennas Propag.*, vol. 66, no. 7, pp. 3295–3305, Jul. 2018.
[12] G. Pan, Y. Li, Z. Zhang, and Z. Feng, "Isotropic radiation from a compact planar antenna using two crossed dipoles," *IEEE Antennas Wireless Propag. Lett.*, vol. 11, pp. 1338–1341, 2012.
[13] C. Deng, Y. Li, Z. Zhang, and Z. Feng, "A wideband isotropic radiated planar antenna using sequential rotated L-Shaped monopoles," *IEEE Trans. Antennas Propag.*, vol. 62, no. 3, pp. 1461–1464, Mar. 2014.
[14] C. Cho, H. Choo, and I. Park, "Broadband RFID tag antenna with quasi-isotropic radiation pattern," *Electron. Lett.*, vol. 41, no. 20, pp. 1091–1092, Sep. 2005.
[15] L. Liang and S. V. Hum, "A low-profile antenna with quasi-isotropic pattern for UHF RFID applications," *IEEE Antennas Wireless Propag. Lett.*, vol. 12, pp. 210–213, 2013.
[16] H. Matzner, M. Milgrom, and S. Shtrikman, "A study of finite size power isotropic radiators," in *Proc. IEEE 18th Conv. Electr. Electron. Eng. Isr.*, Mar. 1995, pp. 1–5.
[17] H. Matzner and K. T. McDonald, "Isotropic radiators," 2003, *arXiv:0312023*. [Online]. Available: http://arxiv.org/pdf/physics/0312023.pdf
[18] H. Matzner and E. Levine, "Can $\lambda/4$ radiators be really isotropic," *Int. J. Antennas Propag.*, vol. 2012, pp. 1–9, Jan. 2012.
[19] H. Matzner, M. Milgrom, and S. Shtrikman, "Magnetoelectric symmetry and electromagnetic radiation," *Ferroelectrics*, vol. 161, no. 1, pp. 213–219, Nov. 1994.
[20] S. Lee, H. Jung, H. Choo, and I. Park, "Design of a U-shaped RFID tag antenna with an isotropic radiation characteristic," in *Proc. IEEE Int. Workshop Antenna Technol., Small Antennas, Novel Struct. Innov. Metamaterials*, Hong Kong, Mar. 2011, pp. 306–309.
[21] S. Lee, H. Jung, H. Choo, and I. Park, "Broadband U-shaped RFID tag antenna with quasi-isotropic radiation Characteristics," in *Proc. Int. Symp. Antennas Propag.*, Jeju, South Korea, 2011, pp. 1–2.
[22] Y. Pan and S. Zheng, "A compact quasi-isotropic shorted patch antenna," *IEEE Access*, vol. 5, pp. 2771–2778, 2017.
[23] Q. Li, W.-J. Lu, S.-G. Wang, and L. Zhu, "Planar quasi-isotropic magnetic dipole antenna using fractional-order circular sector cavity resonant mode," *IEEE Access*, vol. 5, pp. 8512–8525, 2017.
[24] Ansoft. *HFSS 3D Full-Wave Electromagnetic Field Simulation for RF, Wireless, Packaging, and Optoelectronic Design*. [Online]. Available: https://www.ansys.com/products/electronics/ansys-hfss
[25] Z. Zhang, "Choke and ferrite beads," in *Antenna Design for Mobile Devices*, 2nd ed. Hoboken, NJ, USA: Wiley, 2017, pp. 239–243.